



Assessing the interplay between canopy energy balance and photosynthesis with cellulose $\delta^{18}\text{O}$: large-scale patterns and independent ground-truthing

Brent R. Helliker¹ · Xin Song^{1,13} · Michael L. Goulden² · Kenneth Clark³ · Paul Bolstad⁴ · J. William Munger⁵ · Jiquan Chen⁶ · Asko Noormets⁷ · David Hollinger⁸ · Steve Wofsy⁵ · Timothy Martin⁹ · Dennis Baldocchi¹⁰ · Eugenie Euskirchenn¹¹ · Ankur Desai¹² · Sean P. Burns^{14,15}

Received: 18 December 2017 / Accepted: 5 June 2018 / Published online: 28 June 2018
© Springer-Verlag GmbH Germany, part of Springer Nature 2018

Abstract

There are few whole-canopy or ecosystem scale assessments of the interplay between canopy temperature and photosynthesis across both spatial and temporal scales. The stable oxygen isotope ratio ($\delta^{18}\text{O}$) of plant cellulose can be used to resolve a photosynthesis-weighted estimate of canopy temperature, but the method requires independent confirmation. We compare isotope-resolved canopy temperatures derived from multi-year homogenization of tree cellulose $\delta^{18}\text{O}$ to canopy-air temperatures weighted by gross primary productivity (GPP) at multiple sites, ranging from warm temperate to boreal and subalpine forests. We also perform a sensitivity analysis for isotope-resolved canopy temperatures that showed errors in plant source water $\delta^{18}\text{O}$ lead to the largest errors in canopy temperature estimation. The relationship between isotope-resolved canopy temperatures and GPP-weighted air temperatures was highly significant across sites ($p < 0.0001$, $R^2 = 0.82$), thus offering confirmation of the isotope approach. The previously observed temperature invariance from temperate to boreal biomes was confirmed, but the greater elevation of canopy temperature above air temperature in the boreal forest was not. Based on the current analysis, we conclude that canopy temperatures in the boreal forest are as warm as those in temperate systems because day-time-growing-season air temperatures are similarly warm.

Keywords Stable oxygen isotope · Energy balance · Canopy temperature · Leaf temperature · Gross primary production · $\delta^{18}\text{O}$

Introduction

The effect of leaf temperature on photosynthesis is of fundamental importance to plant productivity, distribution, and ecosystem-level carbon and water exchange (Schimper 1903; Walter et al. 1975; Long and Woodward 1988; Larcher 1995), yet because of measurement difficulties, there are few whole-canopy or ecosystem scale assessments of the

interplay between temperature and photosynthesis across both spatial and temporal scales. A combination of abiotic and biotic factors control leaf temperature which can deviate from ambient temperatures through variation in absorbed radiation, transpiration and convective heat loss (Raschke 1960; Gates 1962, 1965; Ehleringer 1989). Variation in biotic factors can cause leaf temperatures to be as much as 10 °C above ambient temperature by leaf clumping, which limits convective heat transfer by increasing the branch-level boundary layer (Smith and Carter 1988) or 18 °C below ambient temperature through evaporative cooling and reduction of absorbed radiation via reflective leaf hairs (Ehleringer et al. 1976; Smith 1978). It is also well-established that optimal leaf temperatures for photosynthetic uptake can vary by species, and shifts with seasonal air temperature (Berry and Bjorkman 1980; Long and Woodward 1988; Michaletz et al. 2016). Simultaneous measurements of whole-canopy or ecosystem scale temperature and photosynthesis has

Communicated by Joy K. Ward.

Electronic supplementary material The online version of this article (<https://doi.org/10.1007/s00442-018-4198-z>) contains supplementary material, which is available to authorized users.

✉ Brent R. Helliker
Helliker@sas.upenn.edu

Extended author information available on the last page of the article

been hindered by measurement difficulties (Miller 1971). Whole-plant photosynthesis systems do exist (Barton et al. 2010), but they necessarily prevent the assessment of canopy energy balance in situ. Thermal-imaging cameras allow for remote, season-long canopy-scale temperature measurements in situ (Leuzinger and Körner 2007; Aubrecht et al. 2016), but to gain information on the relationship between canopy temperatures and carbon uptake, these instruments must be used in concert with eddy-covariance measurements of canopy carbon exchange.

The analysis of the stable oxygen isotope ratio ($\delta^{18}\text{O}$) of plant cellulose represents an integration of canopy energy balance and photosynthesis. The stable isotope ratio of plant cellulose is weighted more heavily by periods of maximal carbon uptake (Farquhar et al. 1989; Cernusak et al. 2005; Gessler et al. 2007), therefore, whatever information that is contained in cellulose $\delta^{18}\text{O}$ is also photosynthesis-weighted. As much as 60% of the $\delta^{18}\text{O}$ of plant cellulose emanates from the $\delta^{18}\text{O}$ of leaf water (Barbour et al. 2000). The enrichment of ^{18}O in leaf water during plant transpiration is controlled in large part by the ratio of ambient water vapor pressure (e_a) to the saturated water vapor pressure at leaf temperature (e_i). With the $\delta^{18}\text{O}$ of water entering a leaf and atmospheric water vapor constant, there is an approximate 0.2‰ change in leaf water $\delta^{18}\text{O}$ for every 0.01 change in e_a/e_i , so the e_a/e_i signal is particularly large. If canopy temperature is equal to air temperature (such that e_i is equal to ambient saturated water vapor pressure), then leaf water $\delta^{18}\text{O}$, and subsequently cellulose $\delta^{18}\text{O}$, can be used to reconstruct relative humidity during a growing season (Saurer et al. 1997, 2000; Anderson et al. 1998; Roden et al. 2000; Robertson et al. 2001; Wright and Leavitt 2006; Porter et al. 2009). If e_a during the period of growth is known, then cellulose $\delta^{18}\text{O}$ can be further deconstructed to obtain a record of e_i . Once e_i is obtained, solving for photosynthesis-weighted canopy temperature is relatively straight forward, because saturated water vapor pressure has a well-established relationship with temperature (Buck 1981).

It has been known for decades that the oxygen isotope ratio of tree cellulose correlates with some component of ambient temperature (Gray and Thompson 1976; Epstein et al. 1977; Yakir 1992), and Helliker and Richter (2008) (Hereafter H&R) further recognized that the $\delta^{18}\text{O}$ of cellulose contains an isotope-resolved, photosynthesis-weighted canopy temperature (hereafter $T_{\text{can}\delta}$). They found a relatively constant value (approximately 21 °C) across tree species of boreal, temperate and subtropical forested biomes, where mean annual temperature (MAT) ranged from −9 to 24 °C. Song et al. (2011) extended the approach to a larger dataset of tree-ring $\delta^{18}\text{O}$ and confirmed the results of H&R showing a narrow range of $T_{\text{can}\delta}$ across boreal, temperate and subtropical biomes, but the $T_{\text{can}\delta}$ of tropical trees were clearly warmer, ranging from 25 to 28 °C, and subalpine

trees much cooler, around 10 °C. Additionally, Flanagan and Farquhar (2014) applied the approach to grasses and found that $T_{\text{can}\delta}$ estimates were similar to those observed via infrared thermometry. These independent data sets confirm that the isotope approach is consistent, but there are still many questions concerning isotopic fractionation factors (Sternberg and Ellsworth 2011), the proportion of the leaf water isotopic signal that is retained in cellulose within a season and across species (Gessler et al. 2009; Song et al. 2014b) and, perhaps most importantly, there is a lack of an independent test on how well $T_{\text{can}\delta}$ matches other measures of canopy photosynthesis and temperature. In short, independent ground-truthing is needed.

Our goal here is to establish an independent comparison of $T_{\text{can}\delta}$ using eddy-covariance data and canopy air temperature that will both test the efficacy of the isotope approach, and coarsely answer some of the hypotheses that emanate from H&R. The relatively small envelope of $T_{\text{can}\delta}$ observed by H&R can have two explanations that are not mutually exclusive: (1) the biophysical and physiological components of tree canopies allow for some degree of homeothermy and (2) canopy temperatures tend to match canopy air temperature, and seasonal averages of canopy temperature weighted by photosynthesis simply do not vary that much across biomes. Ground-truthing of the $T_{\text{can}\delta}$ method to assess these two hypotheses is somewhat problematic because, as detailed above, there are few comparable metrics. We can, however, use eddy-covariance measurements to assess relationships between estimated gross primary productivity (GPP) and canopy-air temperature. This comparison is less than ideal because eddy-covariance provides an ecosystem-scale measurement and isotopes provide measurements on the scale of the individual, but we can gain some measure of efficacy for the isotope approach if there is general agreement between GPP-weighted canopy temperatures and $T_{\text{can}\delta}$.

Methods

Site selection and sampling scheme

From 2009 to 2010 we sampled tree cores from 15 forested eddy-covariance sites; for a subset of these sites, water from stems was extracted for isotope analysis. 13 of the sites approximated the biome distribution used by H&R, and two of the sites were subalpine forests that were chosen as low-temperature growing season sites (Table 1). The sites spanned 34° in latitude and more than 3100 m in elevation. The mean annual temperature (MAT) for the period of study ranged from −3.5 to 20.3 °C. The number of data-years used at each site ranged from 2 to 9, and was determined by the availability of gap-filled, quality-controlled flux data at the time of tree-core sampling.

Table 1 Sites and species within sites used in this study

Ameriflux site	Location	Coordinates	Elevation	Species examined	Years for tree-ring/flux
Austin cary	FL, USA	29.7381, -82.2188	44	Slash pine, <i>Pinus elliottii</i>	2002–2003
Donaldson	FL, USA	29.7547, -82.1633	36	Slash pine, <i>Pinus elliottii</i>	2002–2004
NC loblolly pine	NC, USA	35.8031, -76.6679	12	Loblolly pine, <i>Pinus taeda</i>	2005–2006
Walker branch	TN, USA	35.9588, -84.2874	343	Chestnut oak, <i>Quercus michauxii</i> White oak, <i>Quercus alba</i>	1995–1999
Silas little	NJ, USA	39.9712, -74.4345	48	Pitch pine, <i>Pinus rigida</i> Black oak, <i>Quercus velutina</i>	2005–2006
Niwot ridge	CO, USA	40.0329, -105.5464	3050	Subalpine fir, <i>Abies lasiocarpa</i> engelmann spruce, <i>Picea engelmannii</i> lodgepole pine, <i>Pinus contorta</i> Aspen, <i>Populus tremuloides</i>	1999–2007
GLEES	WY, USA	41.3644, -106.2394	3190	Subalpine fir, <i>Abies lasiocarpa</i> Engelmann spruce, <i>Picea engelmannii</i>	2002–2003
Oak openings	OH, USA	41.5545, -83.8438	230	Black oak, <i>Quercus velutina</i>	2004–2005
Harvard forest	MA, USA	42.5378, -72.1715	340	Red maple, <i>Acer rubrum</i>	2002–2006
Bartlett forest	NH, USA	44.0646, -71.2881	272	Sugar maple, <i>Acer saccharum</i>	2004–2006
Howland forest	ME, USA	45.2041, -68.7402	61	Sugar maple, <i>Acer saccharum</i> Hemlock, <i>Tsuga canadensis</i>	2000–2004
Willow creek	WI, USA	45.806, -90.0798	515	Sugar maple, <i>Acer saccharum</i>	1999–2004
Thompson 1930	MB, Canada	55.9058, -98.5247	257	Black spruce, <i>Picea mariana</i>	2002–2004
Thompson 1964	MB, Canada	55.9117, -98.3822	258	Black spruce, <i>Picea mariana</i>	2002–2004
Fairbanks	AK, USA	63.9198, -145.3781	518	Black spruce, <i>Picea mariana</i>	2010–2011

GPP-weighted canopy air temperature

To develop gross primary productivity (GPP)-weighted estimates of canopy air temperature, we used air temperature, relative humidity (rH) and GPP from the MDS product. GPP is a robust, data-derived quantity (Baldocchi and Sturtevant 2015) and while different methods to resolve GPP result in an approximate 10–15% variance in seasonal to annual GPP, comparisons across sites are robust when a consistent method is used (Desai et al. 2008). The relationship between nocturnal turbulence data and nighttime net ecosystem exchange (NEE) has been analyzed extensively at each site to achieve ecosystem respiration estimates that reflect well-coupled periods. Most sites use a cut-off value for friction velocity (u^* ; m s^{-1}) that results in a near-linear relationship between nighttime NEE and air or canopy temperature, binned by temperature increments at progressively greater values of u^* . For example, the flat, relatively open stands of the Silas Little, NJ site achieve adequate coupling at a friction velocity values $> 0.2 \text{ m s}^{-1}$, while Niwot Ridge, CO has used a values $> 0.4 \text{ m s}^{-1}$.

Sites have then gap-filled nighttime and daytime data using standardized procedures, and summed measured and modeled daytime NEE, and gap-filled nighttime and estimated daytime ecosystem respiration to estimate GPP (Falge et al. 2001; Mofat et al. 2007). Each year of flux and meteorological data from each site was initially analyzed to ensure a complete growing season of data existed. We first determined the growing season

start and end days, which consisted of removing the nighttime periods when $\text{PAR} = 0$, then averaging the GPP for the remaining light periods of each day. The first day of the growing season was determined to be the first day of seven continuous days with an average GPP greater than $1 \text{ g m}^{-2} \text{ s}^{-1}$. The last day of the growing season was determined to be the last day above $1 \text{ g m}^{-2} \text{ s}^{-1}$ before seven continuous days below $1 \text{ g m}^{-2} \text{ s}^{-1}$.

To independently test T_{can6} we developed an ecosystem-based approach that provides a GPP-weighted canopy air temperature (hereafter $T_{\text{a-GPP}}$). To arrive at $T_{\text{a-GPP}}$, we first filtered eddy-covariance data for daytime periods only for the entire study period (2–9 years, depending on the site). At each half-hour time step, GPP was multiplied by ambient air temperature measured at or near canopy height. The sum of these products was then divided by total growing-season GPP to arrive at $T_{\text{a-GPP}}$ (see Eq. 1 below for more details). For three sites, infrared (IR) thermometers (Apogee, Logan, UT, USA) were placed above the canopy to obtain direct canopy temperatures, and these measurements were used to develop GPP-weighted canopy temperatures ($T_{\text{IR-GPP}}$; see Eq. 1 below for more details).

$$T_{\text{GPP}} = \frac{\sum_{i=+\text{GPP}}^N (\text{GPP}_i \times T_{x-i})}{\sum_{i=+\text{GPP}}^N \text{GPP}_i}, \quad (1)$$

Here i is defined by the first period of positive GPP, or the start of the growing season, N equals all half-hour periods

during the growing season with a positive GPP and T_x equals half-hour measures of either ambient air temperatures at canopy height (T_{a-GPP}) or IR-measured canopy temperature (T_{IR-GPP}). We examined the effect of growing season length on our calculated values of T_{a-GPP} for individual years at boreal, subalpine and warm temperate sites by extending and contracting the growing season by 6 days. The largest difference in T_{a-GPP} from our chosen filtering approach was 0.2 °C at the boreal site.

Isotope model description and parameterization

The record of photosynthesis-weighted canopy temperature contained in the stable oxygen isotope ratio ($\delta^{18}O$) of cellulose begins with the enrichment of ^{18}O in leaf water during transpiration. During transpiration, the water molecules containing light isotopes evaporate preferentially, resulting in an enrichment of heavy isotopes in the leaf mesophyll above the isotope ratio of water entering the roots. This enrichment process can be described by the following model developed initially by Craig and Gordon (1965) and modified by Flanagan et al. (1991) and Farquhar and Lloyd (1993),

$$\Delta_e = \varepsilon^* + \varepsilon_K + (\Delta_V - \varepsilon_K) \frac{e_a}{e_i}, \quad (2)$$

where Δ_e is the ^{18}O enrichment of water at the evaporative sites above plant source water (approximated by $\delta^{18}O_e - \delta^{18}O_{source}$). Δ_V is the $\delta^{18}O$ of atmospheric water vapor relative to source water and ε^* is the temperature-dependent equilibrium fractionation factor for the evaporation of water and ε_K is the cumulative kinetic fractionation factor of water vapor diffusing through leaf stomata and the leaf boundary layer (Farquhar and Lloyd 1993). The relative exchange of isotopes between atmospheric water vapor and xylem water is represented by e_d/e_i (Helliker and Griffiths 2007), which is the ambient vapor pressure divided by the saturation vapor pressure at leaf temperature. e_d/e_i can be also viewed as leaf-based relative humidity.

The general model to describe cellulose $\delta^{18}O$ is (Barbour and Farquhar 2000; Roden et al. 2000):

$$\Delta_C = \left(\frac{\Delta_e(1 - e^{-\varphi})}{\varphi} \right) (1 - p_{ex} \times p_x) + \varepsilon_O, \quad (3)$$

where cellulose $\delta^{18}O$ is expressed as an enrichment above source water (Δ_C). The term $[(1 - e^{-\varphi})/\varphi]$ is the Péclet correction and describes the species-specific effect that leaf architecture and water loss have on the balance of enriched evaporative-site water and unenriched vein water in the leaf (Farquhar and Lloyd 1993). The variable p_x represents the proportion of cellulose-synthesis water that is comprised of unenriched water at the site of cellulose-synthesis. The proportion of oxygen atoms in a sucrose molecule that exchange

with this synthesis water is represented by p_{ex} . The equilibrium fractionation factor associated with the exchange of oxygen atoms between carbonyl group and the tissue water is represented by ε_O (Sternberg 1989; Yakir and DeNiro 1990).

To solve for stable isotope-resolved, photosynthesis-weighted canopy temperature ($T_{can\delta}$) we insert Eq. 2 into Eq. 3 and solve for the e_i that satisfies observed Δ_C :

$$e_i = \frac{(\Delta_V - \varepsilon_K) e_a}{\left(\frac{(\Delta_C - \varepsilon_O) \varphi}{(1 - p_{ex} p_x)(1 - e^{-\varphi})} \right) - \varepsilon^* - \varepsilon_K}. \quad (4)$$

Saturated water vapor pressure has a well-quantified relationship with temperature and, therefore, a given saturated vapor pressure yields a unique temperature for e_i (Buck 1981):

$$T_{can\delta} = \frac{240.97 \left(\ln \frac{e_i}{0.61365} \right)}{17.502 - \left(\ln \frac{e_i}{0.61365} \right)}. \quad (5)$$

To populate model predictions for e_i and $T_{can\delta}$ we used $p_x = 1$ (Roden and Ehleringer 1999; Cernusak et al. 2005), $p_{ex} = 0.4$ for angiosperms and $p_{ex} = 0.26$ for gymnosperms based on the work of Song et al. (2014b). It has been reported that p_{ex} may change dynamically within and across species (Gessler et al. 2009; Song et al. 2014a; Cheesman and Cernusak 2017). However, the majority of p_{ex} values have been found to be around 0.4 (Gessler et al. 2014), the value we use for angiosperms. We feel that the work of Song et al. (2014b) justifies the use of $p_{ex} = 0.26$ for gymnosperms, but we did examine the $T_{can\delta}$ in gymnosperms with both p_{ex} values.

Δ_V was assumed to be in equilibrium with source water at the mean growing season temperature (Helliker 2014). We assumed a constant φ of 0.105, yielding a 5% offset from Δ_{LW} (following H&R) such that Eq. 3, the Péclet model, collapses to a two pool model with 5% unenriched water. At each site, e_a was obtained from T_{a-GPP} and from GPP-weighted ambient relative humidity (rH) which is calculated in a manner similar to T_{a-GPP} . We used two approaches for ε_O , we assumed a constant ε_O of 27.2‰ and a temperature-dependent ε_O . The temperature-dependent ε_O was determined from the empirical equation of Sternberg and Ellsworth (2011):

$$\varepsilon_O = 0.0084T^2 - 0.51T + 33.172, \quad (6)$$

where T represents the temperature at which cellulose is synthesized. For this study, we used mean 24 h growing-season air temperature at each site as the value for T .

Sample processing and mass spectrometry measurements

Tree cores were obtained from radially symmetric, dominant tree species (Ramesh et al. 1985) using a 5 mm diameter increment borer (Haglof, Langsele, Sweden). Cores were collected from five trees per species. The cores were sanded lightly to make annual ring boundaries clearly visible. Rings that corresponded to years for which complete flux data were available were removed with an exacto knife under a light microscope. The samples were then homogenized with a Wiley mill and α -cellulose was extracted following the Brendel procedure modified with an addition of 17% NaOH step to remove hemicellulose (Brendel et al. 2000; Gaudinski et al. 2005). 90–100 μ g cellulose samples were weighed into silver capsules. For isotope analysis, cellulose samples were pyrolysed at 1100 °C in a Costech Elemental analyzer. Isotopic composition of the evolved CO gas was determined on a Thermo-Finnigan Delta Plus isotope ratio mass spectrometer, which had a measurement precision of less than 0.23‰ on a standard reference cellulose powder. All cellulose samples were run in triplicate and data were reported on the Standard Mean Ocean Water (SMOW) scale. Tissue water from stem samples was extracted by cryogenic vacuum distillation (West et al. 2006). Water samples (0.5 ml) were analyzed by equilibration for 48 h in 3 ml Exetainer® vials (Labco Limited, UK) with 10/90 mixture CO₂/He. Four replicates of 100 ml of the headspace gas was injected into a gas chromatograph and carried in a helium air stream to a Delta Plus isotope ratio mass spectrometer (Thermo-Finnigan, Germany).

Sensitivity analysis

To examine how errors in measured model inputs affect the calculation of $T_{\text{can}\delta}$, we performed a sensitivity analysis using initial values of $\Delta_C = 30\%$, $T_{\text{air}} = 20$ °C, rH = 50% (assuming ambient rH and leaf-based rH are equal), $\delta^{18}\text{O}_{\text{source}} = -10\%$, $\delta^{18}\text{O}$ water vapor = -19.5% . Offsets for each of these inputs were developed as follows: for the derivation of air temperature and rH errors, we took the mean difference between $T_{\text{a-GPP}}$ and mean daytime air temperature at each site. A similar difference was derived from GPP-weighted rH and mean daytime rH. We chose this method recognizing that most field sites will not be fully equipped with eddy-covariance data to derive $T_{\text{a-GPP}}$ and GPP-weighted rH, but may have nearby weather station data to drive isotope models. This resulted in an air temperature error term of ± 2.6 °C (e.g., air temperature inputs for the sensitivity analysis ranged from 17.4 to 22.6 °C) and rH of $\pm 5.2\%$. For $\delta^{18}\text{O}_{\text{source}}$ and water vapor $\delta^{18}\text{O}_{\text{errors}}$, we took the mean difference between measured and modeled stem $\delta^{18}\text{O}$ and applied this offset (2.7‰) to both stem and

vapor $\delta^{18}\text{O}$. This method was chosen to assess the potential error in $T_{\text{can}\delta}$ that arises from having model-only values and/or being highly incorrect on the parameterization of plant source water $\delta^{18}\text{O}$.

Results

Using either a constant ϵ_{O} of 27.2‰ or the temperature-dependent ϵ_{O} led to very similar site averages for $T_{\text{can}\delta}$ (Fig. 1), with the exception of the subalpine sites where growing-season-air temperatures were comparatively low. Across sites, the average difference between $T_{\text{can}\delta}$ using temperature-dependent versus constant ϵ_{O} was 0.3 °C, and this small difference was driven primarily by the fact that subalpine $T_{\text{can}\delta}$ was 2.8 °C higher when using a constant ϵ_{O} . The relationship of $T_{\text{can}\delta}$ versus MAT was not significant for a constant ϵ_{O} , and was significant for temperature-dependent ϵ_{O} ($F_{1,14} = 4.98$, $p < 0.05$). After removing the subalpine sites, there was no significant relationship with $T_{\text{can}\delta}$ and MAT from temperate to boreal biomes.

To examine the relationship between $T_{\text{can}\delta}$ and $T_{\text{a-GPP}}$ we used the temperature-dependent ϵ_{O} only (Fig. 2). The relationship was highly significant across sites ($F_{1,23} = 99.2$, $p < 0.0001$, $R^2 = 0.82$, $T_{\text{can}\delta} = -3.96 + 1.15T_{\text{a-GPP}}$). Canopy over temperature, the difference between $T_{\text{can}\delta}$ and $T_{\text{a-GPP}}$, had no significant relationships with mean growing season temperatures or MAT across sites, but after removing data from the Niwot Ridge site there was a significant relationship with MAT ($F_{1,19} = 5.3$, $p < 0.05$, $R^2 = 0.22$). Separating results into broad tree-functional types showed that mean gymnosperm $T_{\text{can}\delta}$ was 1.6 °C below $T_{\text{a-GPP}}$, and mean angiosperm $T_{\text{can}\delta}$ was 0.04 °C below $T_{\text{a-GPP}}$. Both of these were biased by the relatively low $T_{\text{can}\delta}$ values at the Niwot Ridge site. When Niwot Ridge was excluded, the gymnosperm $T_{\text{can}\delta}$ was 0.6 °C below $T_{\text{a-GPP}}$ and angiosperm $T_{\text{can}\delta}$ was 0.7 above $T_{\text{a-GPP}}$, but these differences were not significant in either case. When using a $p_{\text{ex}} = 0.4$ for gymnosperms, average gymnosperm $T_{\text{can}\delta}$ was 3.3 °C higher than when using $p_{\text{ex}} = 0.26$, and the relationship to $T_{\text{a-GPP}}$ changed. The mean gymnosperm $T_{\text{can}\delta}$ shifted from 1.6 °C below $T_{\text{a-GPP}}$ to 1.5 °C above $T_{\text{a-GPP}}$ with Niwot Ridge included, and the temperature differences shifted from 0.6 °C below $T_{\text{a-GPP}}$ to 2.9 °C above $T_{\text{a-GPP}}$ with Niwot Ridge excluded.

The reconstruction of $T_{\text{can}\delta}$ was most sensitive to the measured input of $\delta^{18}\text{O}_{\text{source}}$, where errors were as high as 6.5 °C with a 2.7‰ error in $\delta^{18}\text{O}_{\text{source}}$ (Fig. 3). Errors in air temperature of 2.6 °C yield about a 2.8 °C error in calculated $T_{\text{can}\delta}$, and a 5.2% error in rH gives a $T_{\text{can}\delta}$ error of about 1.8 °C. The temperature and rH errors are approximately additive, so using both temperature and rH errors that are +2.6 °C and +5.2% yields a $T_{\text{can}\delta}$ error of 4.6 °C (data not shown). Fortunately, temperature and RH tend to

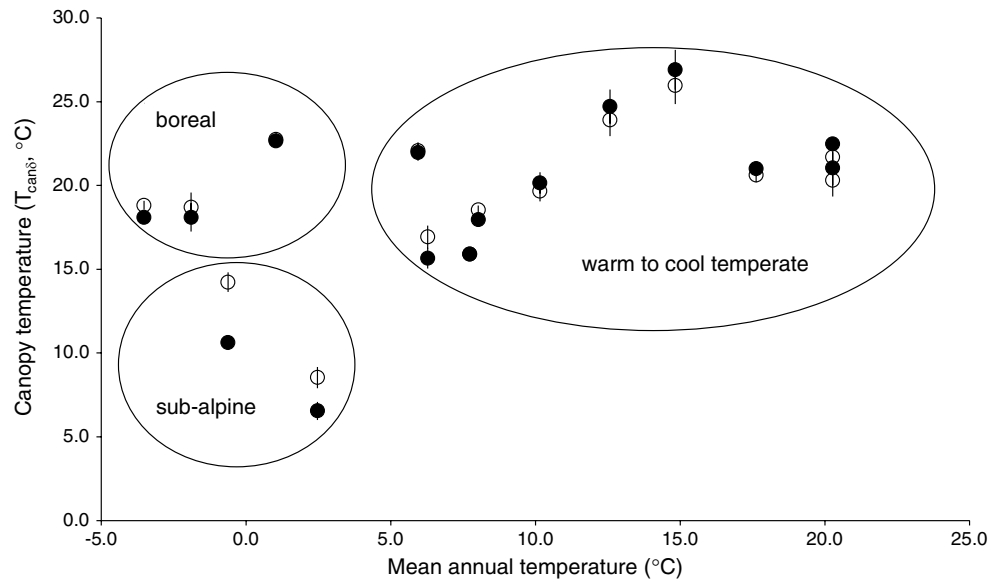
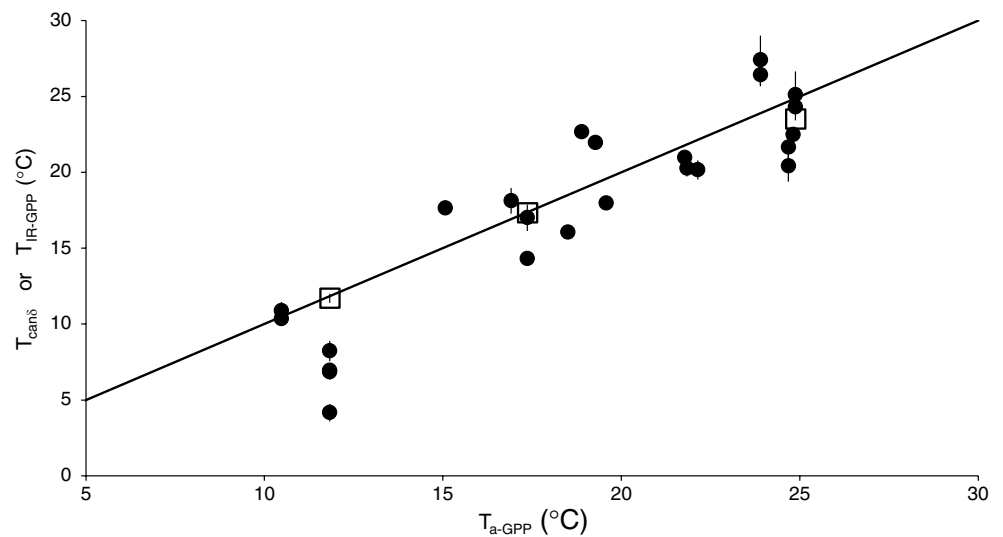


Fig. 1 Site averages for stable oxygen isotope reconstruction of photosynthesis-weighted canopy temperatures ($T_{\text{can}\delta}$). $T_{\text{can}\delta}$ was calculated using both a constant water-to-carbonyl-group fractionation (ϵ_{O})

of 27.2‰ (open circles) and a temperature-dependent ϵ_{O} (closed circles). Error bars represent standard error and are occasionally smaller than the symbol, $n=5$ for each species at each site

Fig. 2 Stable oxygen isotope reconstruction of photosynthesis-weighted canopy temperatures ($T_{\text{can}\delta}$, closed circles) for individual species at each site and GPP-weighted, infrared-derived canopy temperature ($T_{\text{IR-GPP}}$, open squares) vs. GPP-weighted air temperature ($T_{\text{a-GPP}}$). $T_{\text{can}\delta}$ was calculated using a temperature-dependent ϵ_{O} . Error bars represent standard error and are occasionally smaller than the symbol, $n=5$ for each species at each site



be negatively correlated, so that if the temperature used is lower than actual $T_{\text{a-GPP}}$ (as mean daytime growing season temperatures tend to be), then the corresponding rH will be higher than GPP-weighted rH, and the errors tend to offset. This is demonstrated in the final two columns of Fig. 3 where using $T_{\text{air}} + 2.6$ °C and rH -5.2% yields a relatively small error of about 1 °C. Using all errors together does not result in errors much larger than those associated with incorrect $\delta^{18}\text{O}_{\text{source}}$.

We further examined the sensitivity of $T_{\text{can}\delta}$ predictions by focusing on the two similar subalpine sites, Niwot Ridge and GLEES (Table 2). At the GLEES site, model

and observed $\delta^{18}\text{O}_{\text{source}}$ differed by 0.6‰, the standard error of $\delta^{18}\text{O}_{\text{source}}$ was $\pm 1.1\%$, and there was little difference in observed cellulose $\delta^{18}\text{O}$ between tree species (Table 3). For this site, only a temperature-dependent ϵ_{O} was needed for $T_{\text{can}\delta}$ to match $T_{\text{a-GPP}}$ relatively well. For Niwot Ridge, there was a large range in $T_{\text{can}\delta}$ among species that emanated from a 4‰ range in the $\delta^{18}\text{O}$ of cellulose and $\delta^{18}\text{O}_{\text{source}}$. There was also much greater variance in $\delta^{18}\text{O}_{\text{source}}$ at this site ($\delta^{18}\text{O}_{\text{source}}$ standard error as high as $\pm 7.4\%$ in subalpine fir). For the site-level average of $T_{\text{can}\delta}$, modeled $\delta^{18}\text{O}_{\text{source}}$ and a temperature-dependent ϵ_{O} led to the best match with both $T_{\text{a-GPP}}$ and $T_{\text{IR-GPP}}$.

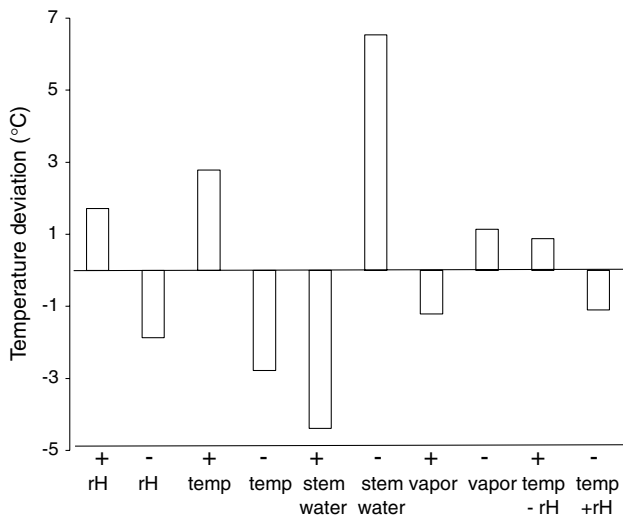


Fig. 3 Sensitivity analysis to examine how errors in model inputs affect the calculation of $T_{\text{can}\delta}$. Initial model inputs were $\Delta_C=30\text{‰}$, $T_{\text{air}}=20\text{ °C}$, $\text{rH}=50\%$, $\delta^{18}\text{O}_{\text{source}}=-10\text{‰}$, $\delta^{18}\text{O}_{\text{water vapor}}=-19.5\text{‰}$. Offsets for each of these inputs were derived from difference in mean growing season data vs. GPP-weighted data, or the difference between observed and modeled isotopic inputs

Discussion

Plant cellulose $\delta^{18}\text{O}$ can be used to reconstruct photosynthesis-weighted canopy temperatures, and we found independent confirmation of the isotope approach with the general agreement between $T_{\text{can}\delta}$, $T_{\text{IR-GPP}}$, and $T_{\text{a-GPP}}$. This agreement further demonstrates a reasonable amount of confidence in our understanding of controls on cellulose $\delta^{18}\text{O}$ across several sites and species. We can provide further confirmation of the isotope approach by examining the match between $T_{\text{can}\delta}$ and modeled values of photosynthesis-weighted canopy temperatures at the Walker Branch site, where we have 19 years of hourly computations using the multi-layered, bio-meteorological model

Canoak (Baldocchi 1997). By being a multi-layer model, the Canoak outputs are analogous to the $T_{\text{can}\delta}$ approach in that both allow for canopy-wide integrations of photosynthesis and temperature. The mean photosynthesis-weighted temperature from Canoak for all 19 years was $22.2 \pm 1.6\text{ °C}$, and a histogram of these photosynthesis-weighted temperatures (presented as a probability density function, Fig. 4) shows a clear peak between 25 and 27 °C. At this site, the $T_{\text{a-GPP}}$ was 23.9 °C and the site mean (tree cores from 1995 to 1999) for $T_{\text{can}\delta}$ was $26.0 \pm 1.1\text{ °C}$.

There are, however, caveats to the agreement between $T_{\text{can}\delta}$ and the other estimated of photosynthesis-weighted canopy temperatures that range from scale comparisons to our knowledge of isotopic inputs and fractionation factors. $T_{\text{a-GPP}}$ and $T_{\text{IR-GPP}}$ are derived in part from eddy-covariance measurements, and therefore, represent an ecosystem-level measure, whereas $T_{\text{can}\delta}$ is derived primarily from measurements on individuals. It is possible that the specific individuals that we measured differed markedly from the aggregate forest in terms of the relationship between canopy temperature, air temperature and photosynthesis. This is unlikely, but it is still a clear shortcoming of the comparison. The fact that GPP-based temperatures were calculated over many years, and $T_{\text{can}\delta}$ was derived from homogenizing tree rings from multiple years, is both a strength and a weakness. It is a weakness largely because we lose any ability to parse out effects that interannual variation in weather may have had on canopy processes. Conversely, it is a strength because by homogenizing tree rings, we smoothed over small-scale variations that would affect isotopic exchange within molecular precursors to cellulose that would affect the value of p_{ex} . These variations can include seasonal or interannual changes in the use of stored versus recently assimilated carbon (Gessler et al. 2009, 2014; Song et al. 2014a, b).

Temperature sensitivity on ϵ_{O} appears to have a muted impact on interpreting cellulose $\delta^{18}\text{O}$ and resolving $T_{\text{can}\delta}$ in most systems. The temperature range over which growth likely occurs in almost all terrestrial plants is well above

Table 2 The sensitivity of $T_{\text{can}\delta}$ predictions to model parameterization at two similar subalpine sites

Site	Niwot Ridge, CO				GLEES, WY				
	Model $\delta^{18}\text{O}_{\text{source}}$, constant ϵ_{O} (°C)	Model $\delta^{18}\text{O}_{\text{source}}$, temp-dependent ϵ_{O} (°C)	Observed $\delta^{18}\text{O}_{\text{source}}$, constant ϵ_{O} (°C)	Observed $\delta^{18}\text{O}_{\text{source}}$, temp-dependent ϵ_{O} (°C)	Tir-gpp (°C)	$T_{\text{a-GPP}}$ (°C)	Model $\delta^{18}\text{O}_{\text{source}}$, constant ϵ_{O} (°C)	Model $\delta^{18}\text{O}_{\text{source}}$, temp-dependent ϵ_{O} (°C)	$T_{\text{a-GPP}}$ (°C)
Lodgepole pine	17.0 ± 1.2	13.4 ± 0.9	8.9 ± 0.6	6.9 ± 0.5					
Subalpine fir	13.3 ± 1.0	10.5 ± 0.8	10.5 ± 0.8	8.2 ± 0.7			13.9 ± 0.4	10.4 ± 0.3	
Englemann’s spruce	11.1 ± 1.0	8.7 ± 0.8	5.8 ± 0.7	4.2 ± 0.6			14.6 ± 0.8	10.9 ± 0.6	
Site mean	13.8 ± 1.0	10.8 ± 0.8	8.4 ± 0.7	6.4 ± 0.6	11.7 ± 0.3	11.8	14.2 ± 0.6	10.6 ± 0.4	10.5

Table 3 Abiotic and isotopic model inputs along with resolved T_{can6} by species for each site

Site	MAT (°C)	Daytime growing season (°C)	24-h growing season temp (°C)	$T_{\text{a-GPP}}$ (°C)	GPP-weighted rH (%)	$\delta^{18}\text{O}_{\text{C}}$ (‰)	$\delta^{18}\text{O}_{\text{source}}$ (‰)	$\delta^{18}\text{O}_{\text{source}}$ modeled	Temp-dependent ϵ_0 (‰)	T_{can6} temp-dependent ϵ_0 (°C)	T_{can6} constant ϵ_0 (°C)
Austin cary pine	20.3	23.2	20.3	24.8	61.3	31.6±0.3	-3.2±1.7	-4.1	26.3	22.5±0.3	21.7±0.3
Bartlett maple	7.7	17.5	16.0	18.5	55.8	27.6±0.2	-7.5±0.8	-10.7	27.2	16.0±0.2	16.0±0.2
Donaldson pine	20.3	23.1	20.3	24.7	60.9	29.1±1.5	-4.1	-4.1	26.3	20.4±1.0	19.7±1.0
Fairbanks b. spruce	-1.9	16.3	14.2	16.9	51.3	21.2±0.7	-20.5	-20.5	27.6	18.1±0.8	18.7±0.9
Florida pine	20.3	23.1	20.3	24.7	60.9	30.7±1.2	-4.1	-4.1	26.3	21.7±1.0	20.9±1.0
GLEES fir	-0.6	8.7	7.6	10.5	46.6	28.0±0.4	-16.3	-16.3	29.8	10.4±0.3	13.9±0.4
GLEES spruce	-0.6	8.7	7.6	10.5	46.6	27.6±0.3	-16.9±1.1	-16.3	29.8	10.9±0.6	14.6±0.8
Harvard maple	8.0	14.8	13.7	19.6	64.8	27.9±0.3	-6.4±0.7	-10.1	27.8	18.0±0.3	18.5±0.3
Howland hemlock	6.3	13.7	11.7	17.4	58.3	27.1±0.5	-9.5±2.3	-10.5	28.4	14.3±0.4	15.3±0.4
Howland maple	6.3	13.7	11.7	17.4	58.3	27.6±0.7	-9.5±2.3	-10.5	28.4	17.0±0.9	18.6±1.0
NC clearcut pine	17.6	17.3	15.9	21.8	60.5	30.3±0.6	-6.3	-6.3	27.2	20.3±0.6	20.3±0.6
NC pine	17.6	17.6	15.9	21.8	60.5	31.1±0.3	-6.3	-6.3	27.2	21.0±0.3	21.0±0.3
Niwot Aspen	2.5	10.2	8.6	11.8	45.0	26.5±0.5	-13.7±1.3	-15.3	29.4	6.9±0.4	9.0±0.5
Niwot Fir	2.5	10.2	8.6	11.8	45.0	28.2±0.7	-13.3±7.4	-15.3	29.4	8.2±0.7	10.5±0.8
Niwot pine	2.5	10.2	8.6	11.8	45.0	30.5±0.6	-9.7±3.2	-15.3	29.4	6.9±0.5	8.9±0.6
Niwot Spruce	2.5	10.2	8.6	11.8	45.0	26.5±0.9	-10.1±3.5	-15.3	29.4	4.2±0.6	5.8±0.7
Ohio oak	10.2	18.7	17.7	22.1	58.5	26.0±0.5	-8.3	-8.3	26.8	20.2±0.6	19.7±0.6
Pine Barrens Oak	12.6	19.9	18.8	24.9	55.4	28.2±1.1	-7.9±1.1	-8.1	26.6	25.1±1.5	24.2±1.4
Pine Barrens pine	12.6	19.9	18.8	24.9	55.4	31.8±0.5	-6.6±0.5	-8.1	26.6	24.3±0.5	23.6±0.5
Thompson 1930 spruce	1.0	17.1	15.6	18.9	56.1	26.0±0.3	-16.3	-16.3	27.3	22.7±0.4	22.8±0.4
Thompson 1964 spruce	-3.5	13.6	12.3	15.1	60.1	25.2±0.2	-16.3	-16.3	28.2	17.6±0.2	18.8±0.3
Walker Br.oak	14.8	21.7	18.4	23.9	59.5	27.8±1.0	-9.7±0.7	-5.9	26.6	27.4±1.6	26.4±1.5
Walker Br. w. oak	14.8	21.7	18.4	23.9	59.5	28.8±0.5	-8.3±0.4	-5.9	26.6	26.4±0.8	25.5±0.7
WillowCreek maple	5.9	16.8	15.5	19.3	62.3	27.2±0.3	-10.5	-10.5	27.3	22.0±0.5	22.1±0.5

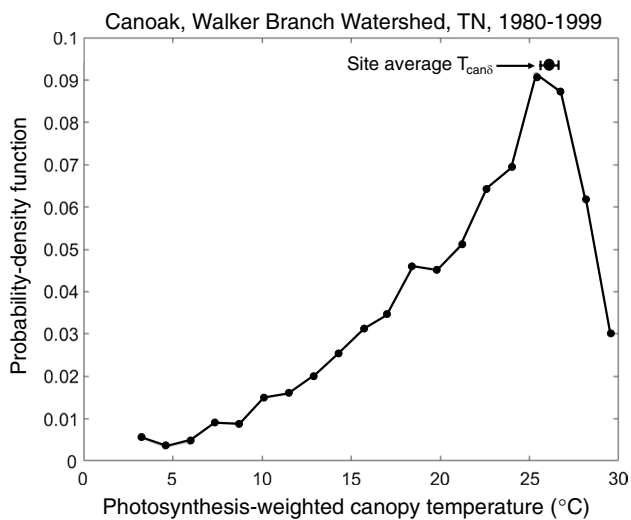


Fig. 4 Histogram of photosynthesis-weighted canopy temperatures (presented as a probability density function) from the multi-layered Canoak model at the Walker Branch site for 19 years of hourly computations. The mean photosynthesis-weighted temperature for all 19 years was 22.2 ± 1.6 °C. The site average $T_{\text{can}\delta}$ for Walker Branch is plotted for comparison

the temperature range for which Sternberg and Ellsworth (2011) found the greatest change in ϵ_O . In applying temperature-based changes in ϵ_O to their interpretation of cellulose $\delta^{18}\text{O}$ across biomes, they assumed that growth occurred at MAT in all systems, and therefore, assumed that growth occurred in the dormant seasons as well as the growing season. Further, they fixed the temperature for ϵ_O at 5 °C for any site with MAT lower than 5 °C, a temperature at which little or no plant growth occurs (Körner 2008). The mean growing-season temperature for each site is the preferable control variable for ϵ_O , because this temperature best reflects seasonal patterns of cambial cell growth and wall thickening (Moser et al. 2010). Excluding the subalpine sites, which will be discussed further below, mean growing season temperature ranged between 11.7 and 20.3 °C at our sites, and the mean temperature-dependent ϵ_O across these sites was $27.3 \pm 0.2\%$. Reanalysis of the Sternberg and Ellsworth data at temperatures between 10 and 25 °C show that there is no significant relationship with temperature, and the mean ϵ_O was 27.8%. Consistent with this, Roden and Ehleringer (2000) found no temperature-induced changes in ϵ_O in *Populus angustifolia* along a transect where mean growing season temperature differences exceeded 5 °C. Lastly, as was pointed out recently (Zech et al. 2014), Sternberg and Ellsworth found a temperature effect on ϵ_O largely because of the a priori assumption that p_{ex} was constant and unaffected by temperature, yet variation in turnover time of the carbohydrate pool—quite possibly associated with temperature—can lead to changes in p_{ex} (Song et al.

2014b). It is worth noting that a temperature-sensitive ϵ_O or p_{ex} would have the same ultimate affect in the final $T_{\text{can}\delta}$ calculation.

Several papers have reported p_{ex} as a variable that may change dynamically in response to changes in environmental or physiological conditions (Gessler et al. 2009; Song et al. 2014a; Cheesman and Cernusak 2017), but the majority of p_{ex} values have been found to be around the value we used here for angiosperms, 0.4 (Cernusak et al. 2005; Gessler et al. 2014). For gymnosperms, we decided to use the $p_{\text{ex}} = 0.26$ for our analyses based on the work of Song et al. (2014b), who compared late wood $\delta^{18}\text{O}_C$ of two oak species and one pine species for 2 years, measuring all isotopic inputs as well as $T_{\text{IR-GPP}}$ for each species. They found that p_{ex} was 0.4 for the angiosperms, but that using a p_{ex} of 0.4 for the pine led to model predictions that were approximately 2.5‰ less enriched than observations. Like several other studies (Szczepanek et al. 2006; Reynolds-Henne et al. 2007; Richter et al. 2008; Roden and Farquhar 2012), Song et al. (2014b) found that pines were more enriched in ^{18}O than co-occurring angiosperms. Direct measurements allowed them to rule out higher canopy temperatures, differences in source-water or leaf water $\delta^{18}\text{O}$, and/or a larger ϵ_O as explanations for the greater enrichment in pine. They concluded that the more enriched $\delta^{18}\text{O}$ of pine was likely due to a lower p_{ex} . A $p_{\text{ex}} = 0.26$ provided the best model-data fit, and was within the range observed for a different pine species by Gessler et al. (2009). When using $p_{\text{ex}} = 0.4$ for gymnosperms in the current study, we found that resolved $T_{\text{can}\delta}$ for gymnosperms were higher than $T_{\text{a-GPP}}$ (in excess of 3 °C when excluding the Niwot Ridge sites), yet the $T_{\text{IR-GPP}}$ estimates of both this study and those of Song et al. (2014b) suggest that, at least with the pines, canopy temperatures matched or were lower than ambient air temperatures. Thus, based on the higher observed $\delta^{18}\text{O}_C$ of gymnosperms that co-occur with angiosperms, the lack of elevated canopy temperatures by direct measurement, and the general energy balance argument that needle-leaved trees should be better coupled to the atmosphere (Jarvis and Mcnaughton 1986), we feel that using a lower p_{ex} for gymnosperms is justified. Whether $p_{\text{ex}} = 0.26$ is the correct number for all gymnosperms, let alone all pine species in all environments, certainly needs further study.

A particularly interesting example of $\delta^{18}\text{O}_{\text{source}}$ error and temperature effects on $T_{\text{can}\delta}$ can be seen by examining the two subalpine sites more closely. For this discussion, we assume that $T_{\text{a-GPP}}$ is the correct target value for $T_{\text{can}\delta}$. GLEES is the simpler scenario because model and observed $\delta^{18}\text{O}_{\text{source}}$ were similar and there was little difference in observed $\delta^{18}\text{O}_C$ between species. For this site, only a temperature-dependent ϵ_O was needed for $T_{\text{can}\delta}$ to match $T_{\text{a-GPP}}$ relatively well. Sternberg and Ellsworth (2011) found the greatest effect on ϵ_O between 5 and 10 °C, and the GLEES

site has a cool growing season, with average 24 h growing season temperature of 7.6 °C, and T_{a-GPP} was 10.5 °C. Niwot Ridge has a similarly cool growing season and similar species to GLEES, yet there was poor agreement in $T_{can\delta}$ among species because both $\delta^{18}O_{source}$ and $\delta^{18}O_C$ were different. Both T_{a-GPP} and T_{IR-GPP} were similar at Niwot Ridge, thus suggesting that resolving $T_{can\delta}$ is highly susceptible to errors in areas where $\delta^{18}O_{source}$ is highly variable. At sites where the $\delta^{18}O$ of precipitation inputs vary greatly through a year, there should be an added focus on sampling source water $\delta^{18}O$ frequently to avoid large errors in $T_{can\delta}$.

The agreement between $T_{can\delta}$ and T_{a-GPP} confirms a similar envelope of photosynthesis-weighted canopy temperatures across warm temperate to boreal biomes shown by H&R, but there are observations in this study that contradict some of the conclusions of H&R. These contradictions revolve around the suggestion that (1) $T_{can\delta}$ invariance can be generalized to forests outside of the range of temperate to boreal forests, and (2) the relationship between canopy temperature to air temperature, or canopy homeothermy. Song et al. (2011) first showed that $T_{can\delta}$ for tropical and subalpine forests was above and below 20 °C, respectively, so the similar finding here is not surprising. The lack of homeothermy suggested here, however, requires greater discussion.

While the same temperature invariance in temperate to boreal biomes observed by H&R was confirmed in this study, the relationship between air temperature and canopy temperature in the boreal forest was not. The large excursion of $T_{can\delta}$ from air temperature in the boreal forests is what drove the discussion of homeothermy in H&R. While we do find a significant relationship between MAT and canopy over temperature ($T_{can\delta} - T_{a-GPP}$), the use of MAT as an independent variable is misleading. It is more appropriate to compare over temperature to mean-growing-season temperature across sites, and for this we find no significant relationship. The over temperature of boreal trees was not systematically greater than other systems. The fact that H&R found that $T_{can\delta}$ was much larger than day-time-growing-season air temperatures in boreal systems than what we found here could be because of the use of weather station air temperatures as opposed to the canopy air temperatures that were used in this study. It is possible that day-time weather station temperatures in the boreal systems are cooler during the day than surrounding forests due to both the lower albedo and lower latent heat exchange in the forests (Baldocchi et al. 2000, Bonan 2008) as compared to cleared areas where standard weather stations are typically located. Such a scenario would certainly have biased the comparisons of H&R. Based on the current analysis, we conclude that canopy temperatures in the boreal forest are as warm as those in temperate systems because day-time-growing-season air temperatures are similarly warm, yet this conclusion does not preclude the possibility of limited homeothermy.

The relationship between leaf and air temperature has been the subject of research for more than 50 years, and while air temperature is clearly the reference point to which leaf temperature tends (Jones 2014), there has long been a question of a systematic deviation from air temperature due to changes in leaf/branch boundary layers or latent heat flux (Gates 1980). Recent work has suggested that plants exist on a continuum of limited homeothermy (Michaletz et al. 2015, 2016; Dong et al. 2017), where leaves can, through adjustment of absorbed radiation, transpiration, convective heat loss and the thermal time constant, maintain an offset above or below air temperature. Our results show that across different sites and species, canopy temperatures do not deviate much from air temperatures when both are photosynthesis-weighted. However, when considering the errors associated with the $T_{can\delta}$ approach—and because we homogenized tree rings across multiple years—our results are too coarse and may be masking small offsets between air and canopy temperatures. To fully examine the existence of limited homeothermy, and perhaps more importantly whether limited homeothermy is adaptive and/or relevant in terms of productivity, it is probably better to examine photosynthesis-weighted canopy temperatures at faster response times using the combination of thermal imagery and eddy-covariance flux measurements.

Photosynthesis and the energy balance of leaves are indelibly linked, yet it has been difficult to obtain measurements in one without precluding the measurement of the other, but it is surely the combination of canopy temperatures and photosynthesis that matters over the long term. We have confirmed here that the stable isotope approach to resolve photosynthesis-weighted canopy temperatures successfully integrates these processes. At the current time, our lack of understanding of small, temporal scale variability in a variety of isotopic fractionation factors and/or within-plant carbon cycling may limit the application of $T_{can\delta}$ to at least annual resolution, and possibly even multi-year integrations as were done here. This still leaves a broad range of open applications, however, such as the examination of plants growing along altitudinal transects or ecotones where climatic changes are most acute, and co-occurring plants with differing life-history strategies.

Acknowledgements BRH would like to acknowledge the intellectually stimulating and unfailingly supportive environment provided by Jim Ehleringer during those young and formative years, despite the ongoing and fruitless quest to locate Baby Jesus. BRH and XS were supported by the National Science Foundation under award number IOS-0950998. The National Center for Atmospheric Research (NCAR) is sponsored by NSF.

Author contribution statement BRH and XS conceived and designed the data collection and modeling approach. BRH, XS, MLG, KC, PB, JWM, JC, AN, DH, SW, TM, DB, EE, AD and SPB collected and


analyzed data. BRH and XS wrote the manuscript; other authors provided editorial advice.

References

- Anderson WT, Bernasconi SM, McKenzie JA, Saurer M (1998) Oxygen and carbon isotopic record of climatic variability in tree ring cellulose (*Picea abies*): an example from central Switzerland (1913–1995). *J Geophys Res* 103:31625–31636
- Aubrecht DM, Helliker BR, Goulden ML, Roberts DA, Still CJ, Richardson AD (2016) Continuous, long-term, high-frequency thermal imaging of vegetation: uncertainties and recommended best practices. *Agric For Meteorol* 228–229:315–326
- Baldocchi D (1997) Measuring and modelling carbon dioxide and water vapour exchange over a temperate broad-leaved forest during the 1995 summer drought. *Plant Cell Environ* 20:1108–1122
- Baldocchi D, Sturtevant C (2015) Does day and night sampling reduce spurious correlation between canopy photosynthesis and ecosystem respiration? *Agric For Meteorol* 207:117–126
- Baldocchi D, Kelliher FM, Black TA, Jarvis P (2000) Climate and vegetation controls on boreal zone energy exchange. *Glob Change Biol* 6:69–83
- Barbour MM, Farquhar GD (2000) Relative humidity- and ABA-induced variation in carbon and oxygen isotope ratios of cotton leaves. *Plant Cell Environ* 23:473–485
- Barbour MM, Fischer RA, Sayre KD, Farquhar GD (2000) Oxygen isotope ratio of leaf and grain material correlates with stomatal conductance and grain yield in irrigated wheat. *Aust J Plant Physiol* 27:625–637
- Barton CVM, Ellsworth DS, Medlyn BE et al (2010) Whole-tree chambers for elevated atmospheric CO₂ experimentation and tree scale flux measurements in south-eastern Australia: the Hawkesbury forest experiment. *Agric For Meteorol* 150:941–951
- Berry J, Bjorkman O (1980) Photosynthetic response and adaptation to temperature in higher plants. *Annu Rev Plant Physiol* 31:491–543
- Bonan GB (2008) Forests and climate change: forcings, feedbacks, and the climate benefits of forests. *Science* 320:1444–1449
- Brendel O, Iannetta PPM, Stewart D (2000) A rapid and simple method to isolate pure alpha-cellulose. *Phytochem Anal* 11:7–10
- Buck AL (1981) New equations for computing vapor pressure and enhancement factor. *J Appl Meteorol* 20:1527–1532
- Cernusak LA, Farquhar GD, Pate JS (2005) Environmental and physiological controls over oxygen and carbon isotope composition of Tasmanian blue gum, *Eucalyptus globulus*. *Tree Physiol* 25:129–146
- Cheesman AW, Cernusak LA (2017) Infidelity in the outback: climate signal recorded in $\Delta^{18}\text{O}$ of leaf but not branch cellulose of eucalypts across an Australian aridity gradient. *Tree Physiol* 37:554–564
- Craig H, Gordon LI (1965) Deuterium and oxygen 18 variations in the ocean and marine atmosphere. In: Tongiorgi E (ed) Stable isotopes in oceanographic studies and paleotemperatures. Consiglio Nazionale Delle Ricerche Laboratorio di Geologia Nucleare, Pisa, pp 9–130
- Desai AR, Richardson AD, Moffat AM et al (2008) Cross-site evaluation of eddy covariance GPP and RE decomposition techniques. *Agric For Meteorol* 148:821–838
- Dong N, Prentice IC, Harrison SP, Song QH, Zhang YP (2017) Biophysical homeostasis of leaf temperature: a neglected process for vegetation and land-surface modelling. *Glob Ecol Biogeogr* 26:998–1007
- Ehleringer JR (1989) Temperature and energy budgets. In: Pearcy RW, Ehleringer JR, Mooney HA, Rundel PW (eds) Plant physiological ecology field methods and instrumentation. Chapman and Hall, London, pp 117–135
- Ehleringer JR, Bjorkman O, Mooney HA (1976) Leaf pubescence: effects on absorbance and photosynthesis in a desert shrub. *Science* 192:376–377
- Epstein S, Thompson P, Yapp CJ (1977) Oxygen and hydrogen isotopic ratios in plant cellulose. *Science* 198:1209–1215
- Falge E, Baldocchi D, Olson R et al (2001) Gap filling strategies for defensible annual sums of net ecosystem exchange. *Agric For Meteorol* 107:43–69
- Farquhar GD, Lloyd J (1993) Carbon and oxygen isotope effects in the exchange of carbon dioxide between terrestrial plants and the atmosphere. In: Ehleringer JR, Hall AE, Farquhar GD (eds) Stable isotopes and plant carbon/water relations. Academic Press, San Diego, pp 47–70
- Farquhar GD, Ehleringer JR, Hubick KT (1989) Carbon isotope discrimination and photosynthesis. *Annu Rev Plant Physiol Mol Biol* 40:503–537
- Flanagan L, Farquhar G (2014) Variation in the carbon and oxygen isotope composition of plant biomass and its relationship to water-use efficiency at the leaf- and ecosystem-scales in a northern Great Plains grassland. *Plant Cell Environ* 37:425–438
- Flanagan L, Comstock J, Ehleringer J (1991) Comparison of modeled and observed environmental influences on the stable oxygen and hydrogen isotope composition of leaf water in *Phaseolus vulgaris* L. *Plant Physiol* 96:588–596
- Gates DM (1962) Energy exchange in the biosphere. Harper and Row, New York
- Gates DM (1965) Energy, plants, and ecology. *Ecology* 46:1–13
- Gates DM (1980) Biophysical Ecology. Springer, New York, p 611
- Gaudinski JB, Dawson TE, Quideau S et al (2005) Comparative analysis of cellulose preparation techniques for use with ¹³C, ¹⁴C, and ¹⁸O isotopic measurements. *Anal Chem* 77:7212–7224
- Gessler A, Peuke AD, Keitel C, Farquhar GD (2007) Oxygen isotope enrichment of organic matter in *Ricinus communis* during the diel course and as affected by assimilate transport. *New Phytol* 174:600–613
- Gessler A, Brandes E, Buchmann N, Helle G, Rennenberg H, Barnard R (2009) Tracing carbon and oxygen isotope signals from newly assimilated sugars in the leaves to the tree-ring archive. *Plant Cell Environ* 32:780–795
- Gessler A, Ferrio JP, Hommel R, Treydte K, Werner RA, Monson RK (2014) Stable isotopes in tree rings: towards a mechanistic understanding of isotope fractionation and mixing processes from the leaves to the wood. *Tree Physiol* 34:796–818
- Gray J, Thompson P (1976) Climatic information from O18/O16 ratios of cellulose in tree rings. *Nature* 262:481–482
- Helliker BR (2014) Reconstructing the $\delta^{18}\text{O}$ of atmospheric water vapour via the CAM epiphyte *Tillandsia usneoides*: seasonal controls on $\delta^{18}\text{O}$ in the field and large-scale reconstruction of $\delta^{18}\text{O}_a$. *Plant Cell Environ* 37:541–556
- Helliker BR, Griffiths H (2007) Toward a plant-based proxy for the isotope ratio of atmospheric water vapor. *Glob Change Biol* 13:723–733
- Helliker BR, Richter SL (2008) Subtropical to boreal convergence of tree-leaf temperatures. *Nature* 454:511–514
- Jarvis PG, McNaughton KG (1986) Stomatal control of transpiration: scaling up from leaf to region. *Adv Ecol Res* 15:1–49
- Jones HG (2014) Plants and Microclimate. Cambridge University Press, Cambridge
- Körner C (2008) Winter crop growth at low temperature may hold the answer for alpine treeline formation. *Plant Ecol Divers* 1:3–11
- Larcher W (1995) Physiological plant ecology. Springer, New York

- Leuzinger S, Körner C (2007) Tree species diversity affects canopy leaf temperatures in a mature temperate forest. *Agric For Meteorol* 146:29–37
- Long SP, Woodward FI (1988) Plants and temperature. The Society for Experimental Biology, Cambridge
- Michaletz ST, Weiser MD, Zhou J, Kaspari M, Helliker BR, Enquist BJ (2015) Plant thermoregulation: energetics, trait–environment interactions, and carbon economics. *Trends Ecol Evol* 30:714–724
- Michaletz ST, Weiser MD, McDowell NG, Zhou J, Kaspari M, Helliker BR, Enquist BJ (2016) The energetic and carbon economic origins of leaf thermoregulation. *Nat Plants* 2:16129
- Miller PC (1971) Sampling to estimate mean leaf temperatures and transpiration rates in vegetation canopies. *Ecology* 52:885–889
- Moffat AM, Papale D, Reichstein M et al (2007) Comprehensive comparison of gap-filling techniques for eddy covariance net carbon fluxes. *Agric For Meteorol* 147:209–232
- Moser L, Fonti P, Buntgen U, Esper J, Luterbacher J, Franzen J, Frank D (2010) Timing and duration of European larch growing season along altitudinal gradients in the Swiss Alps. *Tree Physiol* 30:225–233
- Porter TJ, Pisaric MFJ, Kokelj SV, Edwards TWD (2009) Climatic signals in $\delta^{13}\text{C}$ and $\delta^{18}\text{O}$ of tree-rings from white spruce in the Mackenzie Delta Region, Northern Canada. *Arct Antarct Alp Res* 41:497–505
- Ramesh R, Bhattacharya SK, Gopalan K (1985) Dendroclimatological implications of isotope coherence in trees from Kashmir Valley, India. *Nature* 317:802–804
- Raschke K (1960) Heat transfer between the plant and the environment. *Annu Rev Plant Physiol* 11:111–126
- Reynolds-Henne CE, Siegwolf RTW, Treydte KS, Esper J, Henne S, Saurer M (2007) Temporal stability of climate–isotope relationships in tree rings of oak and pine (Ticino, Switzerland). *Glob Biogeochem Cycles* 21:GB4009
- Richter SL, Johnson AH, Dranoff MM, LePage BA, Williams CJ (2008) Oxygen isotope ratios in fossil wood cellulose: isotopic composition of Eocene- to Holocene-aged cellulose. *Geochim Cosmochim Acta* 72:2744–2753
- Robertson I, Waterhouse JS, Barker AC, Carter AHC, Switsur VR (2001) Oxygen isotope ratios of oak in east England: implications for reconstructing the isotopic composition of precipitation. *Earth Planet Sci Lett* 191:21–31
- Roden JS, Ehleringer JR (1999) Hydrogen and oxygen isotope ratios of tree-ring cellulose for riparian trees grown long-term under hydroponically controlled environments. *Oecologia* 121:467–477
- Roden JS, Ehleringer JR (2000) There is no temperature dependence of net biochemical fractionation of hydrogen and oxygen isotopes in tree-ring cellulose. *Isot Environ Health Stud* 36:303–317
- Roden JS, Farquhar GD (2012) A controlled test of the dual-isotope approach for the interpretation of stable carbon and oxygen isotope ratio variation in tree rings. *Tree Physiol* 32:490–503
- Roden JS, Lin G, Ehleringer JR (2000) A mechanistic model for interpretation of hydrogen and oxygen isotope ratios in tree-ring cellulose. *Geochim Cosmochim Acta* 64:21–35
- Saurer M, Aellen K, Siegwolf R (1997) Correlating $\delta^{13}\text{C}$ and $\delta^{18}\text{O}$ in cellulose of trees. *Plant Cell Environ* 20:1543–1550
- Saurer M, Cherubini P, Siegwolf R (2000) Oxygen isotopes in tree rings of *Abies alba*: the climatic significance of interdecadal variations. *J Geophys Res* 105:12461–12470
- Schimper AFW (1903) Plant-geography upon a physiological basis. Clarendon Press, Oxford, p 839
- Smith WK (1978) Temperatures of desert plants: another perspective on the adaptability of leaf size. *Science* 201:614
- Smith WK, Carter GA (1988) Shoot structural effects on needle temperatures and photosynthesis in conifers. *Am J Bot* 75:496–500
- Song X, Farquhar GD, Gessler A, Barbour MM (2014a) Turnover time of the non-structural carbohydrate pool influences $\delta^{18}\text{O}$ of leaf cellulose. *Plant Cell Environ* 37:2500–2507
- Song X, Clark KS, Helliker BR (2014b) Interpreting species-specific variation in tree-ring oxygen isotope ratios among three temperate forest trees. *Plant Cell Environ* 37:2169–2182
- Song X, Barbour MM, Saurer M, Helliker BR (2011) Examining the large-scale convergence of photosynthesis-weighted tree leaf temperatures through stable oxygen isotope analysis of multiple data sets. *New Phytol* 192:912–924
- Sternberg LSL (1989) Oxygen and hydrogen isotope ratios in plant cellulose: mechanisms and applications. In: Rundel PW, Ehleringer JR, Nagy KA (eds) Stable isotopes in ecological research. Springer, New York, pp 124–141
- Sternberg L, Ellsworth PFV (2011) Divergent biochemical fractionation, not convergent temperature, explains cellulose oxygen isotope enrichment across latitudes. *PLoS One* 6:e28040
- Szczepanek M, Pazdur A, Pawelczyk S et al (2006) Hydrogen, carbon and oxygen isotopes in pine and oak tree rings from southern Poland as climatic indicators in years 1900–2003. *Geochronometria* 25:67–76
- Walter H, Harnickell E, Mueller-Dombois D (1975) Climate-diagram maps of the individual continents and the ecological climatic regions of the Earth. Springer, Berlin
- West AG, Patrickson SJ, Ehleringer JR (2006) Water extraction times for plant and soil materials used in stable isotope analysis. *Rapid Commun Mass Spectrom* 20:1317–1321
- Wright WE, Leavitt SW (2006) Boundary layer humidity reconstruction for a semiarid location from tree ring cellulose $\delta^{18}\text{O}$. *J Geophys Res Atmos* 111:D18105
- Yakir D (1992) Variations in the natural abundance of oxygen-18 and deuterium in plant carbohydrates. *Plant Cell Environ* 15:1005–1020
- Yakir D, DeNiro MJ (1990) Oxygen and hydrogen isotope fractionation during cellulose metabolism in *Lemna gibba* L. *Plant Physiol* 93:325–332
- Zech M, Mayr C, Tuthorn M, Leiber-Sauheitl K, Glaser B (2014) Reply to the comment of Sternberg on “Zech et al. (2014) Oxygen isotope ratios ($^{18}\text{O}/^{16}\text{O}$) of hemicellulose-derived sugar biomarkers in plants, soils and sediments as paleoclimate proxy I: Insight from a climate chamber experiment. *GCA* 126, 614–623”. *Geochimica et Cosmochimica Acta* 141:680–682

Affiliations

Brent R. Helliker¹  · Xin Song^{1,13} · Michael L. Goulden² · Kenneth Clark³ · Paul Bolstad⁴ · J. William Munger⁵ · Jiquan Chen⁶ · Askö Noormets⁷ · David Hollinger⁸ · Steve Wofsy⁵ · Timothy Martin⁹ · Dennis Baldocchi¹⁰ · Eugenie Euskirchenn¹¹ · Ankur Desai¹² · Sean P. Burns^{14,15}

¹ Department of Biology, University of Pennsylvania, Philadelphia, PA, USA

² Department of Earth System Science, University of California, Irvine, CA, USA

- ³ USDA Forest Service, Northern Research Station, New Lisbon, NJ, USA
- ⁴ Department of Forest Resources, University of Minnesota, Saint Paul, MN, USA
- ⁵ Department of Earth and Planetary Sciences, School of Engineering and Applied Sciences, Harvard University, Cambridge, MA, USA
- ⁶ Department of Geography, Center for Global Change and Earth Observations (CGCEO), Michigan State University, East Lansing, MI, USA
- ⁷ Department of Ecosystem Science and Management, Texas A & M University, College Station, TX, USA
- ⁸ USDA Forest Service, Northern Research Station, Durham, NH, USA
- ⁹ School of Forest Resources and Conservation, University of Florida, Gainesville, FL, USA
- ¹⁰ ESPM, University of California, Berkeley, Berkeley, CA, USA
- ¹¹ Institute of Arctic Biology, University of Alaska-Fairbanks, Fairbanks, AK, USA
- ¹² Department of Atmospheric and Oceanic Sciences, University of Wisconsin-Madison, Madison, WI, USA
- ¹³ College of Life Sciences and Oceanography, Shenzhen University, Shenzhen, Guangdong, China
- ¹⁴ Department of Geography, University of Colorado, Boulder, CO, USA
- ¹⁵ National Center for Atmospheric Research, Boulder, CO, USA